Journal of Structural Chemistry. Vol. 50, No. 4, pp. 702-711, 2009

PROCEEDINGS OF THE XIV SEMINAR ON INTERMOLECULAR INTERACTIONS AND MOLECULE CONFORMATIONS

EFFECT OF THE HYDROGEN BRIDGE GEOMETRY ON THE VIBRATIONAL SPECTRA OF WATER: TWO-PARAMETER H-BONDING POTENTIALS

Yu. Ya. Efimov

UDC 532.74

A principle to design the multi-parameter potentials of hydrogen bonding is proposed and developed. Based on fluctuation theory, they provide the description of temperature evolution of the shape of OH vibrational spectra of liquid water molecules. Approximate solutions expressing the ν_{OH} frequency and hydrogen bond energy E through the hydrogen bond length and bending ($R_{O...O}$, $\varphi_{H-O...O}$) and the pair of angles ($\varphi_{H-O...O}$, $\chi_{-O...O}$) adjacent to it are found numerically. By their means, spectra are calculated fairly close to experiment in a temperature range up to 200°C. The expressions proposed can be used to quantitatively analyze the networks of hydrogen bonds in computer models of water obtained by Monte-Carlo or molecular dynamics methods.

Keywords: liquid water, continuum model, hydrogen bond, fluctuation theory, geometry, potential, vibrational spectra.

INTRODUCTION

The structure and unique properties of liquid water are largely based on a spatial three-dimensional network of hydrogen bonds (H-bonds) between OH groups and lone pairs of oxygen atoms of adjacent molecules. These bonds differ in geometrical parameters, the energy and frequency of vibrations of involved oscillators, and in the lifetime of a given pair of molecules as partners in H-bond [1]. The network itself is easily rearranged due to the reorientation of gradually weakening hydrogen bonds (caused by the diffusion of neighbors) towards the partners more favorably located. Current theory and computer simulation methods have already made it possible to describe many properties of water. So, the problem of choice of the most adequate model for its structure from many alternatives, which for decades have been proposed to explain new experimental facts, could have been solved, in principle. However, the interpretation capabilities of these methods are restricted by that the contribution of hydrogen bonds is not identified in the potentials used. So one has to set the existence of the hydrogen bond in a pair of adjacent molecules based on a rather arbitrary yes-no type "threshold" criteria, and the analysis of network topology with regard to the strength of hydrogen bonds (energy "coloring" of the network) is very problematic.

Institute of Chemical Kinetics and Combustion, Siberian Division, Russian Academy of Sciences, Novosibirsk; efimov@kinetics.nsc.ru. Translated from *Zhurnal Strukturnoi Khimii*, Vol. 50, No. 4, pp. 729-738, July-August, 2009. Original article submitted June 21, 2008.

 0022-4766/09/5004-0702

Meanwhile, vibrational spectra are exquisitely sensitive to the hydrogen bond energy. The form of the dependence between the O–H frequency of the water oscillator ν_{OH} involved in H-bond and the energy $E(\nu_{OH})$ is known [2, 3]. Using this fact, here we set a task to find out how this energy (or frequency ν_{OH}) should depend on the main geometrical parameters of a hydrogen bridge (let us denote their ensemble as $\{G\}$) in order to describe the frequency distributions $P(\nu_{OH}, T)$ obtained from the experimental spectra of HOD molecules in the maximum available temperature ranges. It is the sought expression for $E(\{G\})$ that we will call the H-bond potential.

In [4] we have formulated the approach aimed to compare the shape of bands of water OH vibrations with the statistical distribution of geometrical parameters $\{G\}$ of the O–H…O hydrogen bridge in liquid. In order to establish such a relation, we used both purely spectroscopic data and their known empirical correlations with the results of structural studies. The two simplest ideas out of those proposed in the literature to explain the anomalous broadening of spectral bands of associated liquids have been tested, i.e., the dominant effect of the $R_{O...O}$ H-bond length or of the bending angle φ(H–O…O) on the frequency of OH vibrations. We succeeded to strictly solve each of the tasks set, but the obtained relation between the geometrical parameters, frequency of OH vibrations, and the hydrogen bond energy turned out to be in obvious discrepancy with other known data, which indicated insufficiency of the one-parameter approximation for the H-bond potential. In this work, we develop this approach to construct multi-parameter hydrogen bond potentials and to study in detail the cases when its energy simultaneously depends on two geometrical parameters of the hydrogen bridge. The review of the recent literature in this field, a comparison of various models for the water structure as well as detailed motivation of the work and its possible applications are given in the first part of the study [4].

1. CONSTRUCTION OF MULTI-PARAMETER H-BOND POTENTIALS CONSISTENT WITH SPECTROSCOPIC EXPERIMENT

According to the fluctuation theory of hydrogen bonding, the broad bands of stretching vibrations of water molecules in liquid are the result of the statistical distribution of configurations of O–H…O hydrogen bridges [5]. They differ in geometrical parameters and H-bond energies, which leads to different low-frequency shifts of the vibrational frequency of OH groups relative to the unperturbed (without H-bond) value [5, 6]. In the static approximation, the basis of the spectrum of these vibrations at an arbitrary temperature T is represented by the statistical contour $P(\nu)$ well described by the Boltzmann formula [7]

$$P(\nu, T) \sim W(\nu)\exp[-E(\nu)/(k_b T)]. \quad (1)$$

Both of the functions entering it, i.e., the hydrogen bond energy E and the degeneration of states W corresponding to this frequency, are known and are temperature independent [2, 3]. The idea of the approach proposed in [4] is to fill phenomenological formula (1) with structural content, i.e., to express the hydrogen bond energy E and its degeneration W through geometrical parameters of the O–H…O fragment, which generate the frequency ν_{OH} in the spectrum. It is accepted that this frequency is mostly affected by three parameters of the hydrogen bridge: the $R_{O...O}$ length and $\varphi_{H–O...O}$ and $\chi_{–O...O}$ angles between the OH group, and the lone pair with O…O direction respectively. Then in order to solve the problem stated, we need to determine such a dependence of ν (and thereby of E, too) on (R, φ, χ) that would describe temperature evolution of experimental spectra by formula (1) at a reasonably set relation $W(R, \varphi, \chi)$. For this purpose we propose an expression for random occurrence of the triplet of parameters $\{G\} \equiv (R, \varphi, \chi)$ in the O–H…O fragment, corresponding to the volume differential in the space of configurations

$$W(R, \varphi, \chi) = 4\pi R^2 \sin(\varphi)\sin(\chi). \quad (2)$$

It determines a purely geometrical probability for the proton donor OH group of one water molecule to meet the O proton acceptor of another molecule at a distance $R_{O...O}$; the deviation angles of the OH group direction and the oxygen lone pair from the ideal (linear) configuration of the hydrogen bridge would make φ and χ respectively. Therefore, the degeneration of

the hydrogen bridge configuration does not depend, as it must, on the bond energy. The latter determines the total occurrence probability of this configuration at the temperature T by the multiplier $\exp[-E(R, \varphi, \chi)/(k_b T)]$, as in formula (1).

To find the sought dependence $E(R, \varphi, \chi)$, we use the fact that the form of the function $W(\nu)$ we determined quantitatively (see [2, 3]. It is not difficult to numerically find also the integral of this function from the minimum frequency $\nu_{min} \approx 3100$ cm^{-1} [2] occurring in liquid water to an arbitrary value of the frequency ν_{OH} within the statistical contour $P(\nu)$, i.e.,

$$J(\nu_{OH}) \equiv \int_{\nu_{min}}^{\nu_{OH}} W(\nu) d\nu. \quad (3)$$

But in terms of geometrical parameters $\{G\}$ this integral should equal the integral of the function $W(R, \varphi, \chi)$ over the whole range of variables generating a frequency lower than or equal to the upper integration limit ν_{OH} in $J(\nu_{OH})$. Therefore the basic integral equation relating the frequency ν_{OH} to the hydrogen bridge geometry is

$$\int_{G:\nu \le \nu_{OH}} W(G) dG = \int_{\nu_{min}}^{\nu_{OH}} W(\nu) d\nu \equiv J(\nu_{OH}). \quad (4)$$

In other words, the integral of the already known function $W(\nu)$ from zero to any preset value of ν_{OH} should equal the integral of the function $W(G)$ over the definition range involving all combinations of the values of geometrical parameters G corresponding to frequencies $\nu \le \nu_{OH}$.

In [4] we have considered two simplest interpretations of those proposed in the literature for the spectrum nature when the frequency ν_{OH} (and, correspondingly, also the H-bond energy E) depends on the only parameter, i.e., the bond length R [8-10] or its bending angle φ [11, 12]. Here it turns out that equation (4) has strict solutions $\nu_{OH}(R)$ or $\nu_{OH}(\varphi)$ respectively (another matter is that these solutions are physically unsatisfactory). However, if the set G contains several geometrical parameters, integral equation (4) leads to an incorrect inverse problem of searching for the relation $\nu_{OH}(G)$, whose solution requires special approaches and refining (and simplifying) assumptions. We attempted to limit ourselves to the minimum of those required, quite aware of possible imperfections of the solution obtained. First and foremost, the effect of the hydrogen bond length R and both bending angles φ and χ on the low-frequency shift of the frequency ν_{OH} to the unperturbed ("monomeric") value $\nu_u = 3707$ cm^{-1} is assumed to be multiplicative

$$(\nu_u - \nu_{OH}) = \Phi(R) \cdot F(\varphi) \cdot f(\chi). \quad (5)$$

Here the radial dependence $\Phi(R)$ is taken from the empirical correlation [13], where R is expressed in angstroms and frequencies in (5) are given in reciprocal centimeters

$$\Phi(R) = 2.222 \cdot 10^7 \cdot \exp(-3.925R). \quad (6)$$

Then the dependences $F(\varphi)$ and $f(\chi)$ are assumed to be functions monotonically declining from unity to zero with an increase in the corresponding angle from zero (linear hydrogen bond) to limit values φ_{lim} and χ_{lim} causing this bond to break. Thus, for linear H-bonds in liquid, formula (5) reproduces a reduction of the frequency shift with extending (weakening) bond, known from experiments on crystal hydrates [13, 14], while a deviation of the OH group direction and of the lone pair from the linear geometry results in an additional decrease in this shift down to zero (bond breakage, $\nu_{OH} = \nu_u$). Finally, in this work we limit ourselves to the situation when the frequency ν_{OH} depends on two geometrical parameters: (R, φ) or (φ, χ).

1. 1. Potential with two angles. Let the frequency ν_{OH} not depend on the bond length R and be completely determined by its bending angles φ and χ weakening the H-bond (in an interval from the minimum possible for the water–water system $\nu_{min} \approx 3100$ cm^{-1} at $\varphi = \chi = 0$ to $\nu_u = 3707$ cm^{-1} at the limit value of any of the angles).

$$(\nu_u - \nu_{OH}) = (\nu_u - \nu_{min}) \cdot F(\varphi) \cdot f(\chi). \quad (7)$$

With increasing φ and χ the angular H-bond "strength factors" $F(\varphi)$ and $f(\chi)$ decrease from unity to zero. In this case, initial integral equation (4) with taking into account analog (2) acquires the form of

$$J(\nu) = \int_0^{\varphi(\nu)} \sin(\alpha) \int_0^{\chi(\nu,\alpha)} \sin(\beta) d\beta d\alpha, \quad (8)$$

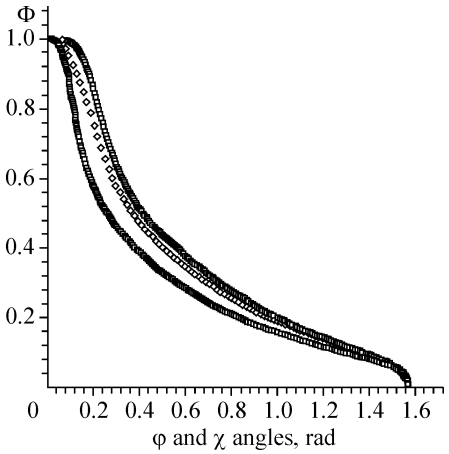

Fig. 1. Lower $\Phi_1(\alpha)$ and upper $\Phi_2(\alpha)$ estimations of the solution region $F(\varphi)\cdot f(\chi)$ of equations (8) and (7), numerically found from the solution of equations (9a) and (9b). The "optimal" solution is between them (10).

where the upper integration limits of $\varphi(\nu)$ and $\chi(\nu, \alpha)$ resrict the range of angles corresponding to frequencies from ν_{min} to the sought $\nu = \nu_{OH}$ in the left part of the equation.

It is worth noting that while in the outer integral the upper limit φ depends only on ν (corresponding to the situation $\chi = 0$), in the inner one it also depends on the current angle value $\varphi = \alpha$. This extremely complicates the problem.

As most of incorrect inverse problems, equation (8) is likely to have no unique solution of $\nu(\varphi, \chi)$. Since the concrete form of functions $F(\varphi)$ and $f(\chi)$ is little known, let us try to limit the range of possible solutions to $\Phi_1(\alpha)$ from below and to $\Phi_2(\alpha)$ from above assuming $F(\varphi)$ and $f(\chi)$ to behave symbately. A rough evaluation of the product $\Phi_1(\alpha) \sim F(\varphi)\cdot f(\chi)$ can be obtained by calculating the dependence between the angle α and the frequency ν from the integral

$$J(\nu) = \int_0^{\alpha(\nu)} \sin^2(\gamma) d\gamma, \tag{9a}$$

which implies the presence of only pairs of equal angles at the H-bond, $\alpha = \varphi = \chi$. A similar evaluation of the upper boundary $\Phi_2(\alpha) \sim F(\varphi)\cdot f(\chi)$ is produced by the double integral with identical upper limits $\alpha(\nu)$ replacing (8)

$$J(\nu) = \int_0^{\alpha(\nu)} \int_0^{\alpha(\nu)} \sin(\gamma)\sin(\beta) d\gamma d\beta. \tag{9b}$$

In both cases, the dependence $\Phi_i(\alpha) = (\nu_u - \nu_{OH})/ (\nu_u - \nu_{min})$ is found by substituting into it the value $\alpha(\nu)$ instead of α, which was obtained from (9a) and (9b) at the given frequency ν in the left part of the equations. Fig. 1 depicts both boundaries of the solution thus found along with the "optimal" solution found experimentally

$$\Phi(\alpha) = \Phi_1(\alpha)/3 + 2\Phi_2(\alpha)/3. \tag{10}$$

The optimal solution was numerically selected by histogram integration (see below). Its criterion was the best description of the experimentally known function $W(\nu)$ of formula (1). The desired solution

$$\Phi(\alpha) = x_1\Phi_1(\alpha) + x_2\Phi_2(\alpha), \quad x_1 + x_2 = 1 \tag{11}$$

was represented by a linear combination of the upper and lower boundaries, while symbasis of the $F(\varphi)$ and $f(\chi)$ behavior in formula (7) was provided by the condition

$$F(\varphi) = (\Phi(\varphi))^a, \quad f(\chi) = (\Phi(\chi))^b, \quad a + b \approx 1. \tag{12}$$

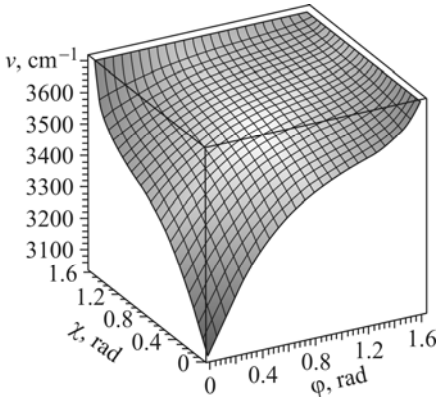

Fig. 2. Dependence of the frequency ν_{OH} on φ and χ angles followed from (14).

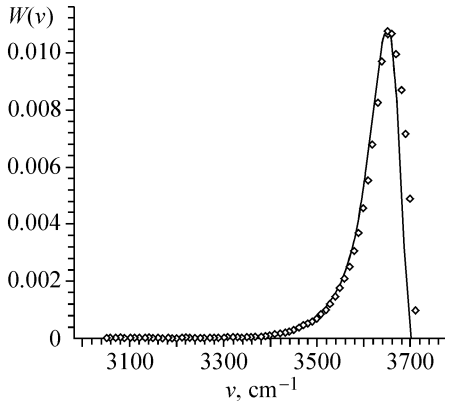

Fig. 3. Dots denote the computer estimation of the function $W(\nu)$ by enumeration of 10^5 pairs of angles (φ, χ) using formula (14); solid line is $W(\nu)$ previously found in [3] from IR spectra of water.

The limiting angles φ_{lim} and χ_{lim} were assumed to be equal to $\pi/2$ for simplicity, which affects only the scale of the axis of angles and, if needed, can be corrected. In the process of histogram integration, the independent pairs of (φ, χ) angles were successively sorted with an equal small step and equal weight within the limits of [0–π/2] each. The product $dW[(\varphi, \chi) \rightarrow \nu_{OH}] = \sin(\varphi)\cdot\sin(\chi)$ was calculated and added to the content of the "box" (channel) of the histogram corresponding to the frequency ν_{OH} calculated by formula (7) for the given pair of angles. So, about 10^5 pairs of angles were sorted in this way, and each of the "boxes" contained the sum of contributions $dW[(\varphi, \chi) \rightarrow \nu_{OH}]$ only from those pairs that generated the frequency $\nu_{OH} \pm 5\text{cm}^{-1}$. The best agreement of thus calculated $W(\nu)$ with experiment was detected at $x_1 = 1/3$, $x_2 = 2/3$; $a = 1/2$, $b = 3/4$ in formulas (11) and (12). For further simplicity of use, the numerical solution for $\Phi(\alpha)$ was approximated by the cubic polynomial

$$\Phi(\alpha) = 1.09 - 2.04\alpha + 1.62\alpha^2 - 0.48\alpha^3, \tag{13}$$

which described the function approximated reasonably well (except the initial part of angles near zero).

The substitution of (12) with regard to (13) into (7) provides the relation between the frequency ν_{OH} and φ and χ angles (Fig. 2), i.e., it solves the problem in the formulation

$$\nu_{OH} = 3707 - (3707 - 3100)\cdot(1.09 - 2.04\varphi + 1.62\varphi^2 - 0.48\varphi^3)^{1/2}\,(1.09 - 2.04\chi + 1.62\chi^2 - 0.48\chi^3)^{3/4}. \tag{14}$$

The found solution of (14) checked by histogram integration shows (Fig. 3) that reconstructured $W(\nu)$ (dots) is in good agreement with the experimental curve (solid line). The observed small discrepancies can be explained by both the approximated character of the solution and imperfect approximation of the function $\Phi(\alpha)$ (13).

In order to calculate the distribution function of φ and χ angles corresponding to the potential given and its temperature dependence (analog of formula (1)) within the fluctuation theory framework

$$P(\varphi, \chi, T) = Q^{-1}(T)\sin(\varphi)\sin(\chi)\exp[-E(\varphi, \chi)/(k_b T)], \tag{15}$$

it is enough to express ν_{OH} through φ and χ using (14) in (16) for the hydrogen bond energy (see [3])

$$E(x) = -0.07x + 0.000104x^2 - 0.493\cdot10^{-6}x^3 + 0.1224\cdot10^{-8}x^4 - 0.828\cdot10^{-12}x^5;$$
$$x = 3707 - \nu_{OH}. \tag{16}$$

Thus calculated pair distributions of angles $P(\varphi, \chi)$ substantially widen with increasing temperature, an obvious shoulder being observed at large angles in the angle distribution $P(\varphi, \chi)$ (orientation of the lone pair). Unfortunately, we are not familiar with the experimental data on the distribution of these angles in liquid water.

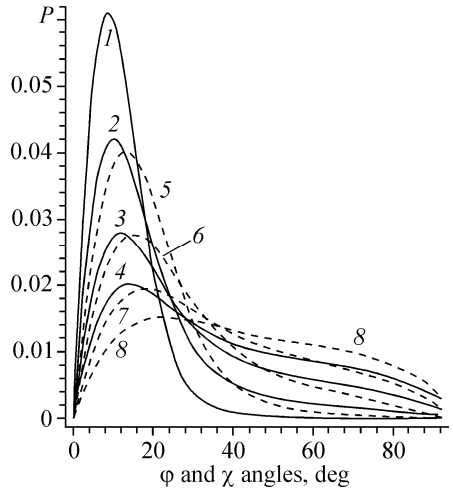

Fig. 4. One-dimensional distribution functions of angles $P(\varphi)$ (solid curves *1-4*) and $P(\chi)$ (dashed curves *5-8*). T –100°C, 0°C, 100°C, 200°C (top-down).

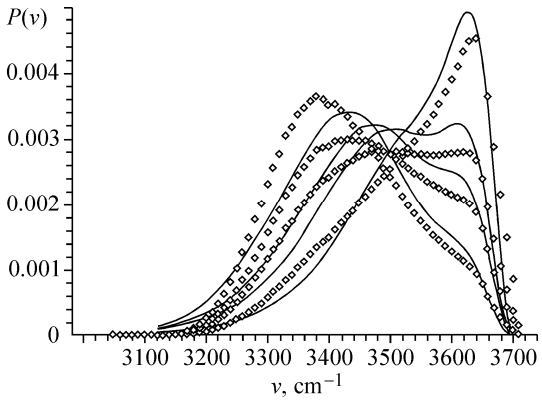

Fig. 5. Distribution of OH vibrational frequencies of water at 0°C, 50°C, 90°C, and 200°C (from left to right). Dots are the calculation (see the text), lines are found from experimental Raman spectra (isotropic component).

Integration of $P(\varphi, \chi)$ surfaces over φ or χ yields traditional one-dimensional distributions of $P(\chi)$ and $P(\varphi)$ angles respectively (Fig. 4). They much more resemble the distributions of the same angles resulted from computer models than those obtained in [4] based on the one-parameter potential $E(\varphi)$.

Finally, the test calculation of the OH vibrational spectra of water molecules within the two-parameter model $E(\varphi, \chi)$ by the formulas of fluctuation theory was carried out similarly to the calculation of the function $W(\nu)$ (Fig. 3). However, in histogram integration, the products by the Boltzmann factor $\exp[-E(\varphi, \chi)/(k_b T)]$ rather than the contributions of different pairs of angles to the degeneration of states $dW[(\varphi, \chi)] = \sin(\varphi)\cdot\sin(\chi)$ were summed in "boxes" for different frequencies, thus giving priority to stronger hydrogen bonds. We have to admit that though the potential obtained does not provide quantitative agreement with experiment, it does provide qualitative agreement (Fig. 5). As in experiment, weak at 0°C the Walrafen shoulder at about 3650 cm^{-1} at 90°C (exactly at 90°!) is comparable in intensity with the low frequency maximum (≈3500 cm^{-1}), and at $T > 100$°C it becomes a dominant component. Within the model given, this can be attributed only to a sharp increase in the fraction of bent hydrogen bonds especially pronounced in evolution of the χ angle distribution (Fig. 4). The model qualitatively correctly describes also the expected behavior of spectra at negative temperatures, i.e., a shift of the maximum to low frequencies, band narrowing, and disappearance of the shoulder of "weak" H-bonds in passing to super-cooled and then to amorphous solid water.

1. 2. Potential with the H bond length and bending angle. We now consider the second version of two-parameter potentials. Let the frequency ν_{OH} (and the H bond energy E) depend on the $R_{O...O}$ bond length and angle φ. Then the purely geometrical (without taking into account the role of energy) probability that the proton-donor H_2O molecule will meet the oxygen atom of the proton-acceptor molecule at a distance of $R \pm dR/2$ at an angle $\varphi \pm d\varphi/2$ relative to the direction of the O–H group is determined by a differential of the conic section area of the spherical layer

$$W(R, \varphi)dRd\varphi = 4\pi R^2 \sin(\varphi)dRd\varphi, \tag{17}$$

and general formula (5) takes the form

$$(\nu_u - \nu_{OH}) = \Phi(R)\cdot F(\varphi), \text{ where } \Phi(R) = 2.222\cdot 10^7 \cdot \exp(-3.925R). \tag{18}$$

Similar to the previous section, the function $F(\varphi)$ should be obtained from the numerical solution of the integral equation, in this case

$$J(\nu) = \int_{R_{min}}^{R(\nu)} r^2 \int_{0}^{\varphi(\nu,r)} \sin(\alpha) d\alpha dr. \quad (19)$$

Here $R(\nu)$ is the maximum $R_{O...O}$ bond length that is still able to yield the frequency ν_{OH} not higher than ν (obviously, at $\varphi = 0$) and is expressed through ν from equation (18) at $F(\varphi) = 1$. From the same equation, the minimum H bond length possible in water R_{min} is found. It corresponds to the low frequency edge of the spectrum ν_{min} in (4).

In order to find $F(\varphi)$, we need to know the dependence $\varphi(\nu, r)$ (the upper limit of the second integral) and to use its "section" at $r = R_{min}$. One would think that only one unknown dependence $F(\varphi)$ in (18) makes the solution of (19) simpler than that of (8) where there are two unknowns. However, we failed to find a satisfactory numerical solution of (19) and (18) with respect to $F(\varphi)$. Therefore it proved better to return to the equation with respect to the function $W(\nu)$ itself instead of its integral $J(\nu)$, thereby reducing the double integral to an ordinary one

$$W(\nu) = \int_{R_{min}}^{R(\nu)} r^2 \sin\varphi(\nu, r) \,|\, \partial\varphi / \partial\nu \,|\, dr. \quad (20)$$

To find the dependence $\varphi(\nu,r)$ entering (20), we use that, according to (18), $F(\varphi)$ can be expressed through ν and r: $F(\varphi) = (\nu_u - \nu)/\Phi(r)$. Knowing that $F(\varphi)$ should be a monotonically declining function from 1 at $\varphi = 0$ to 0 at $\varphi = \varphi_{lim}$, we can employ an artificial technique, representing it from the other side as

$$F(\varphi) = \cos^{x(\nu)}(\pi/2 \cdot \varphi/\varphi_{lim}) \quad (21)$$

with a cosine power depending on the frequency in the right part of equation (21). This makes it possible to alternatively express φ through ν, r, and the auxiliary variable $x(\nu)$ that is to be calculated from (20) at each ν

$$\varphi(\nu, r) = 2\arccos(\exp(\ln F(\varphi)/x(\nu)))\varphi_{lim}/\pi. \quad (22)$$

Since, according to (18), $F(\varphi) = (\nu_u - \nu)/2.222 \cdot 10^7 \cdot \exp(-3.925r)$, then expression (22) has only two independent variables: ν and r. Substituting it into (20), we numerically solve this equation with respect to $x(\nu)$ for discrete ν values from ν_{min} to ν_u. Here the upper integration limit in (20) $R(\nu)$ is assumed to be expressed through ν from equation (18) at $F(\varphi) = 1$, until it reaches the preset value R_{lim}, whereas for higher frequencies it remains equal to R_{lim}. Formally, this restriction is caused by that otherwise the H bond length would tend to infinity with the frequency ν tending to the limit value ν_u, which is impossible in a dense liquid. The physical meaning of the existing limit of the H bond length reflects the fact that at a considerable distance between the partners, the hydrogen bond in water (unlike that in the gas phase) switches to another, more favorable, neighbor. A further increase in the frequency ν_{OH} up to ν_u at $R \approx R_{lim}$ is due to the progressing bending of hydrogen bonds. The necessity of this restriction is also indirectly confirmed by the occurrence of the maximum of the function *W(ν)* (Fig. 3). Otherwise, this value would increase monotonically up to $\nu = \nu_u$ because the weaker the hydrogen bond, the larger is the number of bending and length combinations enabling its occurrence. (Strictly speaking, the R_{lim} value can have no uniform value for all H bonds because conditions for the "switch" of hydrogen bonds can differ in different local environments of a liquid).

We succeeded to find the solutions of (20)-(22) with respect to the auxiliary function $x(\nu)$ almost in the whole range of frequencies, except the 3600-3670 cm^{-1} interval. A very sharp increase in $W(\nu)$ in this region, known from experiment, is likely to be not described in the assumption about multiplicity of bond length and angle contributions (18). Substituting the solution $x(\nu)$ interpolated over the whole frequency range into (21) and assuming in (22) $r = R_{min}$, we find the relation between ν and φ for the strongest (shortest) hydrogen bonds, which at $\varphi = 0$ generate the lowest frequency $\nu_{min} = 3100$ cm^{-1} in the statistical distribution $P(\nu_{OH})$. This allows the behavior of $F(\varphi) = (\nu_u - \nu)/(\nu_u - \nu_{min})$ to be calculated for the given value $r = R_{min}$. However, according to the assumption about the independent effect of R and φ on frequency shift (18), it should be also correct for all the other of bond lengths.

To reveal the role of limit parameters R_{lim} and φ_{lim} in H bond breakage the above calculations were made for four combinations at $R_{lim} = 3.1$ Å and 3.3 Å and $\varphi_{lim} = 60°$ and 90°. It turns out that if the difference in R_{lim} principally affects the

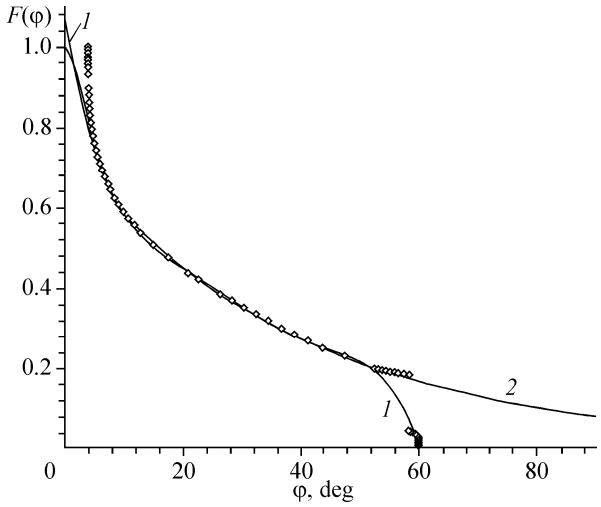

Fig. 6. Approximation of the numerically found angular factor of hydrogen bond weakening $F(\varphi)$ (points) by formulas (23a) (curve *1*) and (23b) (curve *2*). R_{lim} = 3.1 Å, φ_{lim} = 60°.

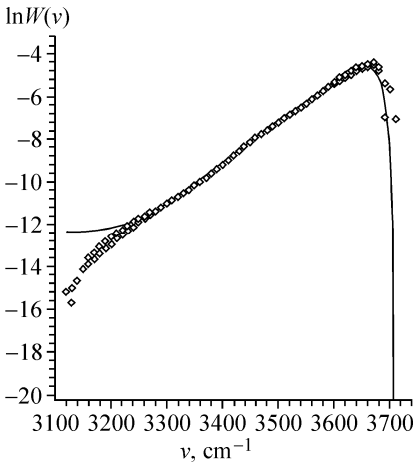

Fig. 7. Logarithm of the function $W(\nu)$ calculated from the spectroscopic experiment (solid line). Dots represent the calculation by formulas (18) and (23a) as well as (18) and (23b).

solution, the role of the φ_{lim} angle can be well taken into account by simple scaling of the axis of angles. If the curves calculated for φ_{lim} = 60° were extended 1.5 times (90°/60°), they would almost coincide with those for φ_{lim} = 90° for both R_{lim} values.

The obtained solutions $F(\varphi)$ were analytically approximated in two ways, namely by the 5th order polynomial running to zero at $\varphi = \varphi_{lim}$ and by the sum of two exponents that monotonically declines to zero at larger angles (Fig. 6). In the case R_{lim} = 3.1 Å, φ_{lim} = 60° these approximations are as follows:

$$F_1(\varphi) = 1.07 - 0.088\varphi + 0.00556\varphi^2 - 0.1906\cdot10^{-3}\varphi^3 + 0.3144\cdot10^{-5}\varphi^4 - 0.1978\cdot10^{-7}\varphi^5, \quad (23a)$$

$$F_2(\varphi) = \exp(-0.3 - 0.025\varphi) + 0.259\exp(-0.035\varphi^2). \quad (23b)$$

Substitution of formulas (23a) or (23b) into (18) sets two versions of the dependence between the frequency ν_{OH} and the H bond length and bending angles, whereas the subsequent use of formula (16) determines the dependence of the H bond energy on these parameters.

The proof of the approximations found for the inverse problem solution by calculating the function $W(\nu)$ (direct problem; the way described above) does not give serious grounds to prefer any of them (Fig. 7). The distributions of hydrogen bond geometrical parameters corresponding to the model given are determined by the expression

$$P(R, \varphi, T) = Q^{-1}(T)R^2\sin(\varphi)\exp[-E(R, \varphi)/(k_bT)], \quad (24)$$

where $Q(T)$ is the statistical integral (statistical sum) in the usual meaning, normalizing distribution (24) at the given temperature T.

The one-dimensional functions of φ angle distributions (Fig. 8) are similar in form and temperature behavior to those calculated with the potential $E(\varphi, \chi)$ (Fig. 4). Their 1.5 times "compression" along the axis of angles is explained by that in the potential $E(\varphi, \chi)$ the angle of H bond breakage was thought to be 90°, while in Fig. 8 the calculation results with φ_{lim} = 60° are given.

The functions of bond length distributions $P(R)$ obtained by integrating (24) over φ are much broader than those obtained in the one-parameter approximation of the potential $E(R)$ [4]. Their shape does not depend on the type of approximating angular dependence of potential (23a) or (23b). However, they still radically differ from the experimental radial distribution functions (RDF) of water by the absence of the maximum of distribution. The reason for this is clear:

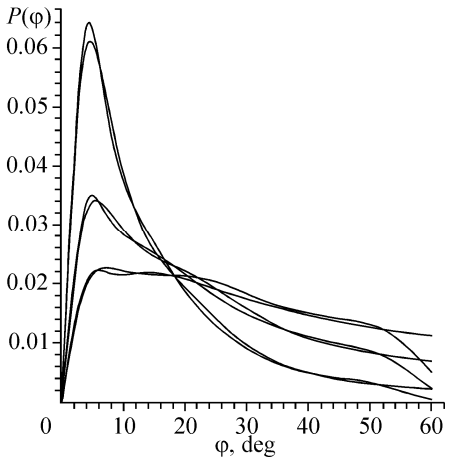

Fig. 8. One-dimensional distribution functions of angles $P(\varphi)$ obtained by integration of two-dimensional distributions $P(R, \varphi, T)$ (formula 24) over R. $T = 0$°C, 100°C, 200°C (from top downwards). Formula (18) and approximations $F(\varphi)$ (23a) (at large angles decline more sharply) and (23b) are used.

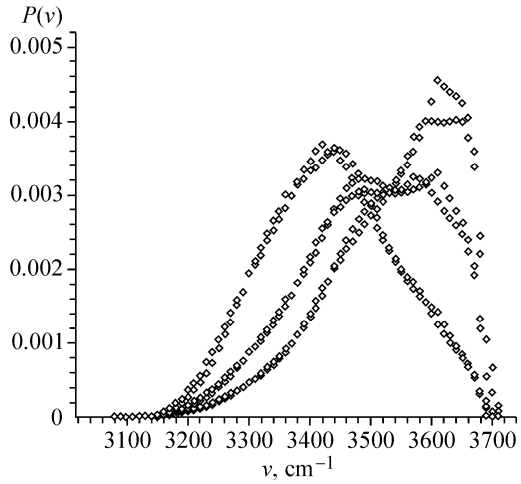

Fig. 9. Distributions of OH vibrational frequencies of water at 0°C, 100°C, and 200°C (from left to right) calculated based on the potential $E(R, \varphi)$ with two approximations of the angular factor $E(R, \varphi)$: polynomial (23a) and the sum of two exponents (23b).

the absence of repulsive (van der Waals) terms in the radial part of the potential. This is the principal difference of the hydrogen bond potential that we developed from the full potentials of intermolecular interactions used in computer simulations. Being inappropriate for simulating the liquid structure, it is intended to quantitatively describe the properties of separate hydrogen bonds and their systems (networks) in computer models already elaborated with the full potential of interaction. Finally, the OH vibrational spectra of water molecules calculated based on the two-parameter model $E(R, \varphi)$ by two of its approximations (Fig. 9) agree with experiment almost as well as those calculated using $E(\varphi, \chi)$ (Fig. 5).

CONCLUSIONS

The problem of possible interdependence between geometrical and spectroscopic parameters of the hydrogen bond and its energy is considered. By numerical calculations, an approximate solution of the incorrect inverse problem on the relation between the spectral frequency ν_{OH} and the geometry of the O–H…O fragment is found for the case when it (or the H-bond energy) depends on the $R_{O...O}$ H-bond length and the bending φ angle. Similarly, we obtained the solution for the case when the pair of significant geometrical parameters consisted of two angles: between the O…O vector and the OH group of a proton-donor molecule and the lone pair of a proton-acceptor molecule respectively. Analytical approximations of the solutions obtained are proposed. The dependences $E(R, \varphi)$ and $E(\varphi, \chi)$ found were tested by calculations of the OH vibrational spectra of water molecules in terms of fluctuation theory of hydrogen bonding. The calculated envelopes of vibrational spectra describe correctly not only the features of the shape of experimental spectra but also their highly characteristic temperature evolution. At the next stage of the study, we plan to generate molecular dynamic models of liquid water in a wide temperature range, to list the geometrical parameters of O–H…O fragments for pairs of the nearest-neighbor molecules, and to use our dependences of the OH vibrational frequency on these parameters to plot the envelope of vibrational spectra following from these models. Under conditions of mathematical incorrectness of the problem considered (the absence of an unambiguous solution), the comparison of spectra calculated in this way with experimental data will help

to refine the features of the dependences discussed. It is not excluded that this comparison will reveal a need to construct a hydrogen bond potential $E(R, \varphi, \chi)$ involving all three geometrical parameters of hydrogen bridge (5).

The work was supported by RFBR grant No. 07-03-00503-a.

REFERENCES

1. G. G. Malenkov, *J. Struct. Chem*., **47**, Suppl., S1-S31 (2006).
2. Yu. Ya. Efimov and Yu. I. Naberukhin, *Mol. Phys*., **101**, 459-468 (2003).
3. Yu. Ya. Efimov and Yu. I. Naberukhin, *J. Struct. Chem*., **41**, No. 3, 433-439 (2000).
4. Yu. Ya. Efimov, *ibid*., **49**, No. 2, 261-269 (2008).
5. Yu. Ya. Efimov and Yu. I. Naberukhin, *Farad. Discuss. Chem. Soc*., **85**, 117-123 (1988).
6. J. D. Smith, Ch. D. Cappa, K. R. Wilson, et al., *Proc. Natl. Acad. Sci. USA*, **102**, 14171-14174 (2005).
7. A. P. Zhukovskii, *Zh. Strukt. Khim*., **17,** 931/932 (1976).
8. T. T. Wall and D. F. Hornig, *J. Chem. Phys*., **43**, 2079-2087 (1965).
9. H. Torii, *J. Phys. Chem. A*, **110**, 9469-9477 (2006).
10. C. P. Lawrence and J. L. Skinner, *J. Chem. Phys*., **118**, No. 1, 264-272 (2003).
11. J. A. Pople, *Proc. Roy. Soc*., **A205**, 163-178 (1951).
12. A. P. Zhukovskii, L. V. Shurupova, and A. M. Zhukovskii, *J. Struct. Chem*., **36**, No. 3, 426-431 (1995).
13. Yu. Ya. *Efimov*, *ibid*., **32**, No. 6, 834-841 (1991).
14. M. Falk, *Chemistry and Physics of Aqueous Gas Solutions*, W. B. Adams et. al. (eds.), Electrochem. Soc. Inc., Princeton (1975), pp. 19-41.